Polyhedron 28 (2009) 679–688

Contents lists available at ScienceDirect

Polyhedron

journal homepage: www.elsevier.com/locate/poly

Construction of metal–organic frameworks with transitional metals based on the 3,5-bis(4-pyridyl)-1*H*-1,2,4-triazole ligand

Xiao-Feng Xie, San-Ping Chen, Zheng-Qiang Xia, Sheng-Li Gao *

Key Laboratory of Synthetic and Natural Functional Molecule Chemistry of Ministry of Education, Department of Chemistry, Northwest University, Xi'an, Shaanxi 710069, China

ARTICLE INFO

Article history:
Received 10 October 2008
Accepted 12 December 2008
Available online 3 February 2009

Keywords:
3,5-Bis(4-pyridyl)-1*H*-1,2,4-triazole (Hbpt)
In situ metal/ligand reaction
Coordination complex
Benzenedicarboxylate ligand
X-ray diffraction

ABSTRACT

Based on the versatile ligand 3,5-bis(4-pyridyl)-1*H*-1,2,4-triazole (Hbpt) derived from an in situ metal/ligand reaction, a series of coordination compounds $CoCl_4(H_3bpt)(H_2O)$ (**1**), $Cu(H_2bpt)_2(SO_4)_2(H_2O)_6$ (**2**), $[Ag(bpt)]_n$ (**3**), $[Co(Hbpt)(pa)]_n$ (**4**), $[Co(Hbpt)(pda)]_n$ (**5**) and $[Cu(Hbpt)(pda)(H_2O)]_n$ (**6**) have been constructed (pa = phthalate, pda = 1,3-phenylenediacetate). The structures of these targeted complexes have been characterized by X-ray single-crystal diffraction techniques. Structural analysis reveals that Hbpt adopts versatile coordination modes to arrange the metal ions in 0-D point, simple (4,4) layers and dinuclear core chains in **1**–**3**, which are further extended via the benzenedicarboxylate connectors to give rise to a variety of coordination networks such as (4,4), $(4^{12}\cdot 6^3)$, $(6^4\cdot 8^2)$ topologies in **4**–**6**. The supramolecular organization through hydrogen bonds is analyzed for these complexes and thermal stability of these crystalline materials has been explored by TG-DTG.

1. Introduction

In coordination and supramolecular chemical fields, metal–organic frameworks (MOFs) have intrigued great interest for their potential application in catalysis, gas absorption, non-linear optics, ion-exchange, luminescence, magnetism and many other fields [1–7]. In principle, the design and syntheses of metal–organic networks via the self-assembly of metal ions and multifunctional ligands greatly depend on the organic ligands (spacers) and metal ions (nodes). Linear 4,4′-bipyridine(4,4′-bpy) and 4,4′-bipyridine-like N,N′-donor ligands are often used as spacers to form open metal–organic frameworks [8–11]. Through introducing moieties between the two 4-pyridyl groups, several couples of bent N,N′-donor ligands, such as 2,5-bis(4-pyridylethynyl) thiophene and 4-amino-3,5-bis(4-pyridyl)-1,2,4-triazole, have been used as building blocks to extend metal–organic frameworks [12–17]. Here we introduce the 1*H*-1,2,4-triazole moiety between the two 4-pyridyl groups due to the following considerations. First, it can act as a bridge between metal centers, thus mediating exchange coupling, and represents a hybrid of pyrazole and imidazole with regard to the arrangement of its three heteroatoms thus promising a rich and versatile coordination chemistry. Second, the prototropy and conjugation between the 1*H*-1,2,4-triazole and 4-pyridyl groups not only alter the electron density in different parts of the molecule, but also make the ligand more flexible, in addition, the wide application in spin-crossover materials and pharmacologically active compounds also makes this moiety more attractive [18–20]. Benzenedicarboxylate species such as phthalate (pa), isophthalate (ip), 1,3-phenylenediacetate (pda) and terephthalate (tp) are widely used in the construction of MOFs, because of their abilities to form non-covalent cooperative forces such as hydrogen bonding and/or aromatic stacking, and to compensate the charge for the neutral ligand [21–24].

Nowadays in situ metal/ligand reactions show great merit in both coordination chemistry and organic synthesis [25,26]. Herein, by using a coordination compound as an intermediate, 3,5-bis(4-pyridyl)-1*H*-1,2,4-triazole has been synthesized via an in situ metal/ligand reaction.

With this understanding, one crucial aim of this work is to explore the introduction effect of 1*H*-1,2,4-triazole for tuning the structural assembly, which may provide further insights in designing new hybrid crystalline materials. In the present work, we report the synthesis of Hbpt and six new coordination polymers, namely $CoCl_4(H_3bpt)(H_2O)$ (**1**), $Cu(H_2bpt)_2(SO_4)_2(H_2O)_6$ (**2**), $[Ag(bpt)]_n$ (**3**), $[Co(Hbpt)(pa)]_n$ (**4**), $[Co(Hbpt)(pda)]_n$ (**5**) and $[Cu(Hbpt)(pda)(H_2O)]_n$ (**6**). The compounds have been structurally determined by single-crystal X-ray diffraction, and characterized by IR and TG-DTG.

2. Experimental

2.1. Materials and analytical methods

All of the reagents were commercially available without further purification. C, H, N contents were determined on a Vario EL III

* Corresponding author.
E-mail address: gaoshli@nwu.edu.cn (S.-L. Gao).

0277-5387/$ - see front matter © 2009 Elsevier Ltd. All rights reserved.
doi:10.1016/j.poly.2008.12.046

analyzer. IR spectra were recorded on a Tensor 27 spectrometer (Bruker Optics, Ettlingen, Germany). All NMR spectra were measured on a Varian INOVA 400 MHz spectrometer. Thermogravimetric analysis was performed on a Netzsch STA 449C simultaneous TGA with a heating rate of 10 °C min^{-1} under nitrogen.

2.2. Syntheses and characterization

2.2.1. 3,5-Bis(4-pyridyl)-1H-1,2,4-triazole (Hbpt)

The Hbpt ligand was synthesized via an in situ metal/ligand reaction and demetallation as followed (Scheme 1): a mixture of 4-cyanopyridine (1.04 g, 10.0 mmol), aqueous ammonium (2.0 mL), $CuSO_4 \cdot 5H_2O$ (0.249 g, 1.0 mmol) and water (5 mL) in a 20-mL Teflon-lined autoclave was treated at 140 °C for 72 h. The resulting mixture was filtered to give crystalline $[Cu_2(bpt)_2]$ in 40% yield based on 4-cyanopyridine.

The product then underwent a process of demetallation: the powder was placed in a 200 mL flask containing 100 mL water, into which 2 mL ammonium sulfide was dropped with stirring. After 0.5 h the solution became dark, and then was boiled to make CuS crystallize out completely. It was then filtered to give a colorless solution and concentrated to afford 3,5-bis(4-pyridyl)-1*H*-1,2,4-triazole (Hbpt) (390 mg, 35% based on 4-cyanopyridine) as a white powder.

Mp 296–297 °C; IR (cm^{-1}, KBr): 3408(w), 3088(m), 2623(m), 1606(s), 1580(s), 1447(m), 1423(m), 1378(m), 1362(m), 1152(s), 1015(m), 987(m), 832(s), 720(m), 709(m), 528(s); ^1H NMR (400 MHz, DMSO-d_6, δ ppm): 8.010–8.025 (4H, d, J = 4.4 Hz), 8.768–8.779 (4H, d, J = 4.4 Hz), 15.232 (1H, s, Triazole-H); *Anal.* Calc. for $C_{12}H_9N_5$: C, 64.56; H, 4.06; N, 31.37. Found:C, 64.63; H, 4.19; N, 32.00%.

2.2.2. $CoCl_4(H_3bpt)(H_2O)$ (**1**)

$CoCl_2 \cdot 6H_2O$ (0.047 g, 0.2 mmol) was added to a methanol solution (10 mL) of Hbpt (44.6 mg, 0.2 mmol) with stirring. The resulting solution was filtered and kept at room temperature for crystallization. After 10 days, light blue crystals of **1** suitable for an X-ray crystallographic study were obtained in a yield of 27% (based on Co). *Anal.* Calc. for **1** ($C_{12}H_{13}Cl_4CoN_5O$): C, 32.46; H, 2.95; N, 15.77. Found: C, 32.41; H, 2.87; N, 15.76%. IR (cm^{-1}, KBr): 3404(w), 3085(m), 2617(m), 1636(m), 1606(w), 1570(s), 1445(s), 1374(m), 1366(m), 1154(s), 1045(m), 967(m), 812(s), 710(m), 521(s).

2.2.3. $Cu(H_2bpt)_2(SO_4)_2(H_2O)_6$ (**2**)

The same synthetic procedure as that for **1** was used except that $CoCl_2 \cdot 6H_2O$ was replaced by $CuSO_4 \cdot 5H_2O$, and blue block X-ray-quality crystals were obtained in a yield of 27% (based on Cu). *Anal.* Calc. for **2** ($C_{24}H_{32}CuN_{10}O_{14}S_2$): C, 35.49; H, 3.97; N, 17.24. Found: C, 35.57; H, 3.88; N, 16.98%. IR (cm^{-1}, KBr): 3409(w), 3085(m), 3019(w), 2617(m), 1626(w), 1570(s), 1426(s), 1374(m), 1366(m), 1154(s), 1017(m), 967(m), 840(s), 736(m), 521(s).

2.2.4. $[Ag(bpt)]_n$ (**3**)

A solution of Hbpt (4.46 mg, 0.020 mmol) in MeOH (10 mL) was carefully layered onto a solution of $AgNO_3$ (3.40 mg, 0.020 mmol) in H_2O (10 mL). The solution was left for 6 days at room temperature, and colorless crystals were obtained in a yield of 78% (based on Ag). *Anal.* Calc. for **3** ($C_{12}H_8AgN_5$): C, 43.66; H, 2.44; N, 21.22. Found: C, 43.54; H, 2.60; N, 21.34%. IR (cm^{-1}, KBr): 3502(w), 3321 (w), 1635(s), 1375(vs), 1532(w), 1482(w), 1307(s), 1215(m), 1037(w), 834(s), 735(w).

2.2.5. $[Co(Hbpt)(pa)]_n$ (**4**)

A mixture containing $Co(OAc)_2 \cdot 4H_2O$ (24.9 mg, 0.10 mmol), Hbpt (22.3 mg, 0.10 mmol), H_2pa (16.6 mg, 0.10 mmol) and water (6 mL) was sealed in a 20 mL Teflon-lined stainless steel vessel, which was heated at 140 °C for 3 days and then cooled to room temperature at a rate of 5 °C/h. Red prism crystals of **4** were collected in a yield of 55% (based on Co). *Anal.* Calc. for **4** ($C_{20}H_{15}CoN_5O_5$): C, 51.74; H, 3.26; N, 15.08. Found: C, 51.65; H, 3.31; N, 15.15%. IR (cm^{-1}, KBr): 3345(s), 3260(s), 1643(w), 1604(s), 1550(s), 1485(s), 1461(s), 1403(s), 1378(s), 1225(m), 1038(w), 1060(w), 1020(s), 995(m), 952(w), 839(m), 771(m), 731(m), 704(s), 604(s), 508(m).

2.2.6. $[Co(Hbpt)(pda)]_n$ (**5**)

The same synthetic procedure as that for **4** was used except that H_2pa was replaced by H_2pda, and red prismatic crystals of **5** were collected in a yield of 50% (based on Co). *Anal.* Calc. for **5** ($C_{22}H_{17}CoN_5O_4$): C, 55.71; H, 3.61; N, 14.76. Found: C, 55.65; H, 3.58; N, 14.85%. IR (cm^{-1}, KBr): 3332(s), 1635(s), 1615(s), 1581(m), 1544(s), 1456(s), 1399(s), 1220(m), 1036(w), 917(w), 836(s),740(s), 720(s), 615(m), 521(m), 433(m).

2.2.7. $[Cu(Hbpt)(pda)(H_2O)]_n$ (**6**)

The same synthetic procedure as that for **5** was used except that $Co(OAc)_2 \cdot 4H_2O$ was replaced by $Cu(OAc)_2 \cdot 4H_2O$, and blue prismatic crystals of **6** were collected in a yield of 57% (based on Cu). *Anal.* Calc. for **6** ($C_{22}H_{19}CuN_5O_5$): C, 53.17; H, 3.85; N, 14.09. Found: C, 53.22; H, 3.88; N, 14.14%. IR (cm^{-1}, KBr): 3410(w), 1635(s), 1605(s), 1575(m), 1537(s), 1404(s), 1378(s), 1235(m), 1112(w), 1032(w), 910(w), 854(s),735(s), 700(s), 613(m), 523(m), 444(m).

2.3. Crystal structure determination and structure refinement

All diffraction data for complexes **1–6** were collected on a Bruker/Siemens Smart Apex II CCD diffractometer with graphite monochromated Mo Kα radiation (λ = 0.71073 Å) at 293(2) K. Cell parameters were retrieved using SMART [27] software and refined using SAINTPLUS [28] for all observed reflections. Data reduction and correction for Lp and decay were performed using the SAINTPLUS software. Absorption corrections were applied using SADABS [29]. All structures were solved by the direct methods using the SHELXS program of the SHELXTL-97 [30] package and refined with SHELXL. Metal atoms in all the complexes were located from the E-maps and other non-hydrogen atoms were located in successive difference Fourier syntheses. The final refinements were performed by full-matrix least squares methods with anisotropic thermal parameters for non-hydrogen atoms on F^2. The H atoms of triazole and pyridyl(N) in Hbpt were located from difference Fourier maps, all other hydrogen atoms were included in calculated positions and refined with isotropic thermal parameters riding on those of the parent atoms. The oxygen atoms (O(1), O(2)) of pda anions in **6** are disordered and an occupancy ratio of 0.6:0.4 was found. Details of the data collection and refinement are given

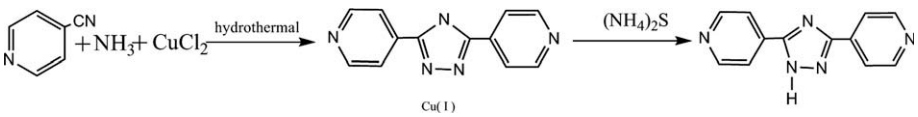

Scheme 1. In situ synthesis of the Hbpt ligand.

Table 1
Crystal data for **1–6**.

	1	2	3	4	5	6
Formula	$C_{12}H_{13}Cl_4CoN_5O$	$C_{24}H_{32}CuN_{10}O_{14}S_2$	$C_{12}H_8AgN_5$	$C_{20}H_{15}CoN_5O_5$	$C_{22}H_{17}CoN_5O_4$	$C_{22}H_{19}CuN_5O_5$
Formula weight	444.00	812.26	330.10	464.30	474.34	496.46
Crystal system	monoclinic	triclinic	monoclinic	triclinic	monoclinic	monoclinic
Space group	*Cc*	$P\bar{1}$	$P2_1/c$	$P\bar{1}$	C_2/c	C_2/c
a (Å)	11.951(3)	7.108(2)	7.609(2)	8.006(4)	24.347(7)	17.779(4)
b (Å)	18.004(3)	8.365(2)	11.332(3)	10.491(5)	10.291(3)	11.958(3)
c (Å)	8.303(2)	14.786(3)	12.944(4)	12.987(6)	16.337(5)	20.137(4)
α (°)	90	73.586(4)	90	66.922(9)	90	90
β (°)	94.423	88.270(4)	104.414(6)	80.276(9)	90.854(6)	97.473(5)
γ (°)	90	67.658(3)	90	68.379(9)	90	90
V (Å^3)	1781.2(7)	777.1(3)	1081.0(6)	932.5(8)	4093(2)	4245(2)
Z	4	1	4	2	8	8
D_{calc} (g cm^{-3})	1.656	1.736	2.028	1.654	1.540	1.554
F(000)	892	419	648	474	1944	2036
R_{int}	0.0425	0.0235	0.0489	0.0844	0.0948	0.0657
Goodness-of-fit on F^2	0.958	0.841	0.997	1.171	0.916	1.130
R_1[a], wR_2[b] [$I > 2\sigma(I)$]	0.0356, 0.0515	0.0449, 0.1268	0.0379, 0.1128	0.1130, 0.2433	0.0473, 0.0536	0.0579, 0.1223
R_1[a], wR_2[b] [all data]	0.0605, 0.0566	0.0660, 0.1558	0.0717, 0.1224	0.2043, 0.2656	0.1275, 0.0617	0.1221, 0.1347
Largest difference in peak/hole (e Å^{-3})	0.264 and −0.304	0.725 and −0.838	0.454 and −0.660	1.146 and −1.599	0.398 and −0.343	0.767 and −0.551

[a] $R_1 = \sum(|F_O| - |F_C|)/\sum|F_O|$.
[b] $R_2 = \{\sum[w(F^2_O - F^2_C)^2]/\sum w(F^2_O)^2]\}^{1/2}$.

in Table 1, selected bond lengths and angles are tabulated in Table S1 and selected hydrogen-bonding geometries for **1**, **2**, **4**, **5** and **6** are listed in Table S2. Further details are provided in the Supplementary data.

3. Results and discussion

3.1. Syntheses of the compounds and IR spectroscopy

3,5-Bis(4-pyridyl)-1*H*-1,2,4-triazole (Hbpt) can be considered as a new member of the group of five-membered heterocyclic ring bridging organic ligands. Compared with other widely investigated N,N′-bipyridine-type ligands, Hbpt is endowed with more structural information, especially for the diverse configurations of the protons on the N atoms. The nitrogen atoms of Hbpt are potential acceptors and donors for hydrogen bonds to expand polymeric frameworks. Interestingly, in the MOFs **1–6**, the ligand exhibits four different states: bpt^-, Hbpt, H_2bpt^+ and H_3bpt^{2+}, which results in the formation of abundant hydrogen bonds (Scheme 2). It is worth noting that ammonium sulfide is an excellent agent for the demetallation of the copper complex. The current approach provides a novel facile route to synthesize this kind of compound.

Three synthetic approaches were applied to construct these coordination polymers. With regard to MOFs **4–6**, they were prepared under hydrothermal conditions, whereas assemblies of the others were carried out under aqueous conditions or using diffusion. In each synthetic case, an approximate metal/ligand composition of 1:1:1/1:1 was utilized for the starting materials. Coordination polymers **1–6** are air stable with the maintenance of their crystallinity for at least several weeks.

In the IR spectra of complexes **1**, **2** and **6**, the broad band centered at 3400 cm^{-1} indicates the O–H stretching of the aqua molecules. The absorption band resulting from the skeletal vibrations of the aromatic rings for all three complexes appears in the 1400–1600 cm^{-1} region. In complexes **4–6**, the characteristic bands of the dicarboxylate groups unit are found at 1610 and 1490 cm^{-1} for asymmetric stretching and 1380 cm^{-1} for symmetric stretching. The strong bands between 1640 and 1630 cm^{-1} and near 1037 cm^{-1} are assignable to the characteristic bands of 1,2,4-triazole. All these spectral features are consistent with the crystal structures as described below.

3.2. Descriptions of crystal structures

3.2.1. Structure of $CoCl_4(H_3bpt)(H_2O)$ (**1**)

As shown in Fig. 1 **1** contains one H_3bpt^{2+} ion, one $[CoCl_4]^{2-}$ ion and one lattice water (Fig. 1). The cobalt cation is coordinated by four chloride anions, which forms a tetrahedral structure. The average Co–Cl bond length is 2.28 Å and the Cl–Co–Cl bond angles are in the range 104.75(6)–112.45(6)°, which are close to the ideal tetrahedral value and are in good agreement with the previously reported bond lengths and angles of a tetrahedral cobalt compound [31]. The Hbpt ligand is protonated by two protons which are attached to the two terminal N atoms (N4, N5). All the three N–H groups (include triazole-H) interact with the chlorides and the water molecule, forming many hydrogen bonds, with O···Cl distances of 3.203(5), 3.106(5), N···Cl distances of 3.222(4), 3.257(5) and N···O distances of 2.700(6), 3.173(3) Å (Fig. 2, Table S2). As is well-known, a water molecule has two hydrogen atoms and two lone-electron pairs, which enables it to participate in four

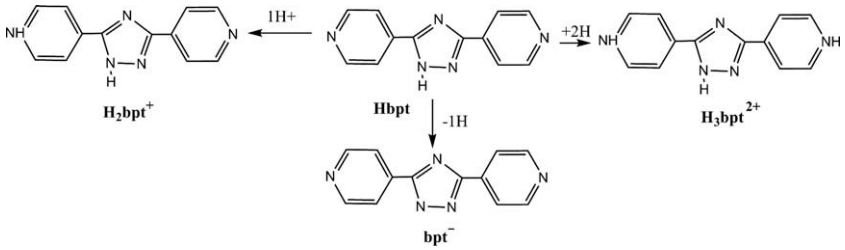

Scheme 2. Different forms of the Hbpt ligand in **1–6**.

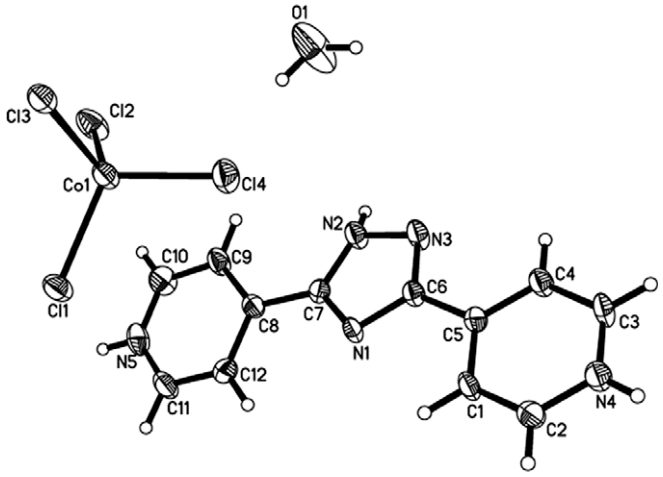

Fig. 1. Thermal displacement diagrams (30%) for **1**.

hydrogen bonds in a tetrahedral configuration, but it also frequently shows a 3-coordinate configuration [32]. In **1**, the lattice water O1 also shows a 3-coordinate mode. Through these hydrogen bonds, the molecule is assembled into a three-dimensional structure (Fig. 2).

3.2.2. Structure of $Cu(H_2bpt)_2(SO_4)_2(H_2O)_6$ (**2**)

Compound **2** consists of a discrete centrosymmetrical $[Cu(H_2bpt)_2(H_2O)_4]^{4+}$ cation, two $[SO_4]^{2-}$ anions and two lattice water molecules, it is more accurate to describe the complex as $[Cu_{0.5}(H_2bpt)(H_2O)_2](SO_4)(H_2O)$. The crystal structure of the cationic mononuclear unit is depicted in Fig. 3. The Cu^{II} ion is located at a crystallographic inversion center, and six coordinated to four aqua ligands in the equatorial plane, as well as two H_2bpt^+ ligands in axial positions. To the two N atoms in the terminal pyridyl (N1, N5) of Hbpt ligand, N5 is coordinated to Cu, while the other is saturated with a proton, forming a +1 cation. The coordination geometry of the metal center can be described as a slightly distorted octahedron with O–Cu–N and O–Cu–O angles in the range

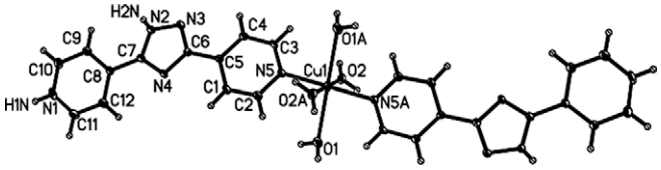

Fig. 3. Thermal displacement diagrams (30%) for **2** ($[Cu(H_2bpt)_2(H_2O)_4]^{4+}$ cation).

86.41(6)–93.59(6)°. The two pyridine rings within each ligand form dihedral angles of 10.03 and 3.42°, respectively, with the central triazole plane, and a dihedral angle of 8.59° with each other.

Herein the Hbpt ligand uses only one of the pyridyl nitrogen atoms to bind the metal center. The other uncoordinated pyridyl nitrogen serves as the hydrogen bond donor to the sulfate anions with a O···N distance of 2.696(4) Å. In the S_4 tetramer of the coordinated aqua molecules (the tetramer of water can be defined as having S_4 symmetry), every monomer acts as a donor for the oxygen atoms from the sulfate ion. The lattice water O7 also serves as a hydrogen bond donor to form two hydrogen bonds with N4 from Hbpt and O4 from the sulfate ions, resulting in a $R_2^2(8)$ ring [33]. All the water molecules show a 2-coordinate configuration hydrogen bond. It is noteworthy that the four oxygen atoms of the sulfate ion form seven different hydrogen bonds with the Hbpt, coordinated water and lattice water. A $R_4^4(12)$ hydrogen bond ring is formed by the two adjacent sulfate anions and two coordinated water molecules (Fig. 4b) [33]. In **2**, the sulfate anions act as a binder extending the block $Cu(H_2bpt)_2(SO_4)_2(H_2O)_6$ into a three-dimensional network by mass hydrogen bonds (Fig. 4a).

3.2.3. Structure of $[Ag(bpt)]_n$ (**3**)

Single-crystal analysis of **3** reveals (Fig. 5) that the Ag^I lies in a trigonal planar (sum of N–Ag–N angles = 359.97°) coordination environment, which consists of two $N_{triazole}$ donors (N(3)–Ag(1) = 2.303(5) and Ag(1)–N(2) = 2.214(5) Å) from two $Hbpt^-$ ligands (the Hbpt ligand loses $H_{triazole}$ forming the bpt^- ion) and one $N_{pyridyl}$ donor (Ag(1)–N(1) = 2.254(5) Å) from the third Hbpt ligand. The Ag–$N_{triazole}$ bond length is considerably longer than those of the Ag–$N_{pyridyl}$ bonds, but all the Ag–N bond distances in

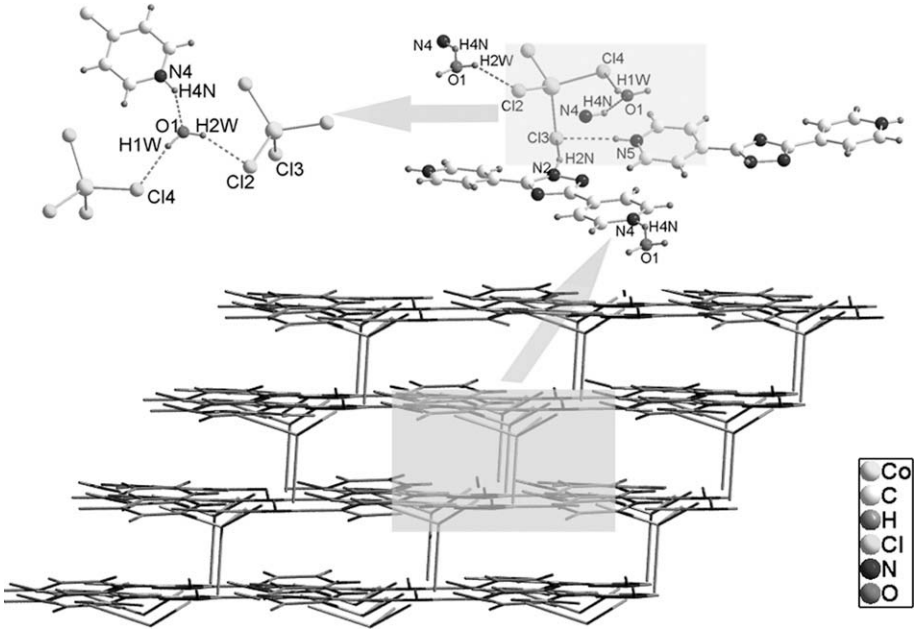

Fig. 2. The supramolecular structure formed by hydrogen bonds (H-bonds: dashed lines) for **1**.

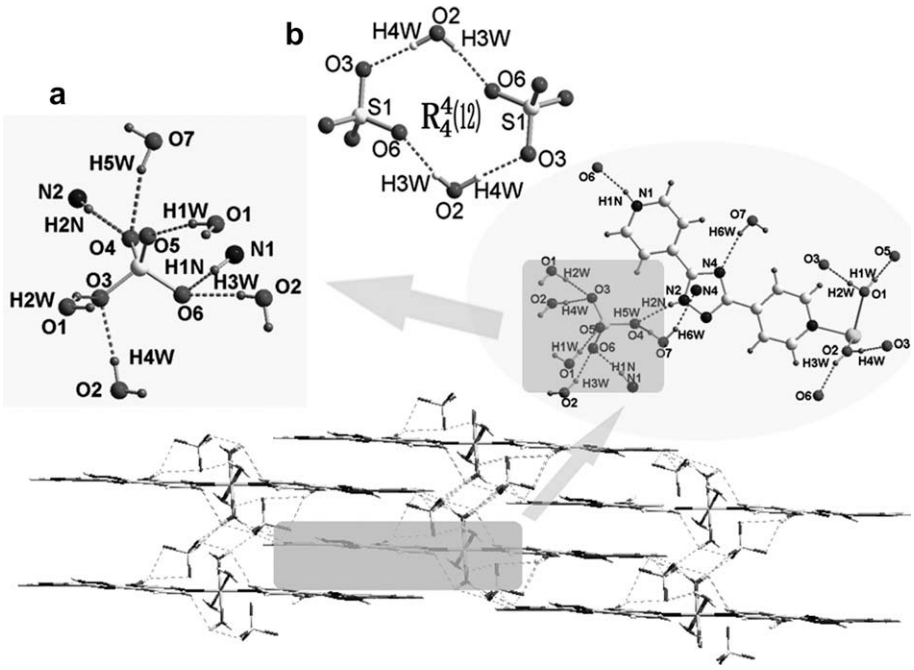

Fig. 4. (a) The supramolecular structure formed by hydrogen bonds (H-bonds: dashed lines) for **2**. (b) The R_4^4 (12) ring.

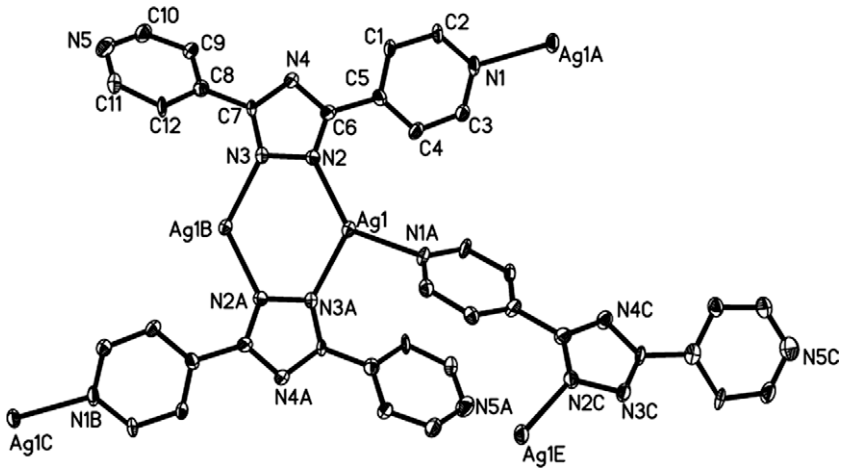

Fig. 5. Thermal displacement diagrams (30%) for **3**.

3 are within the normal range for N-containing heterocyclic Ag(I) complexes [17,34,35]. Each ligand is bonded to three Ag(I) centers (N1–Ag1A, N2–Ag1, N3–Ag1B). Interestingly, the two similar $N_{pyridyl}$ atoms of the Hbpt ligand have very different coordination behavior: N1 coordinates to one Ag atom while the N5 does not. Two Ag(1) atoms are bridged by four $N_{triazole}$ atoms into a dinuclear core with a short Ag···Ag contact of 3.492 Å (Fig. 6), which reveals the existence of an attractive metallophilic interaction [36,37]. The ligand itself is not planar, the corresponding dihedral angles between the three rings are [N(1)···C(5)]–[N(2)···N(3)] = 14.11°, [N(1)···C(5)]–[N(5)···C(12)] = 45.95° and [N(2)···N(3)]–[N(5)···C(12)] = 33.54°.

In the solid state, the Ag(I) centers and bpt^- ligands are linked together into a novel two-dimensional sheet, which is parallel to the [1 1 0] plane. As shown in Fig. 7, the single net mainly consists of a large ring. The large ring comprises a tetrameric unit, in which four Ag(I) centers are linked together by bpt^- ligands into an elliptical 32-membered macrocycle. While the two uncoordinated

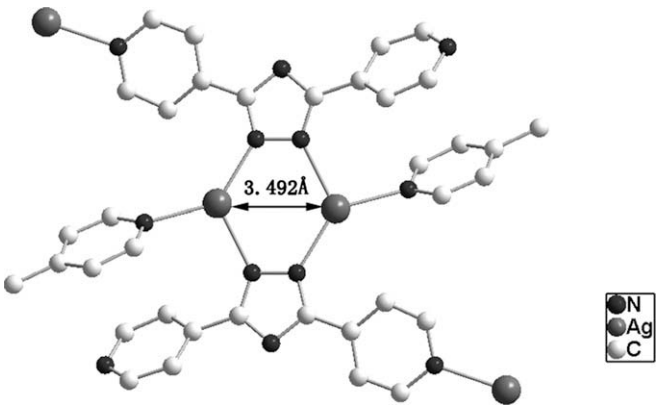

Fig. 6. Short Ag···Ag contacts in compound **3**.

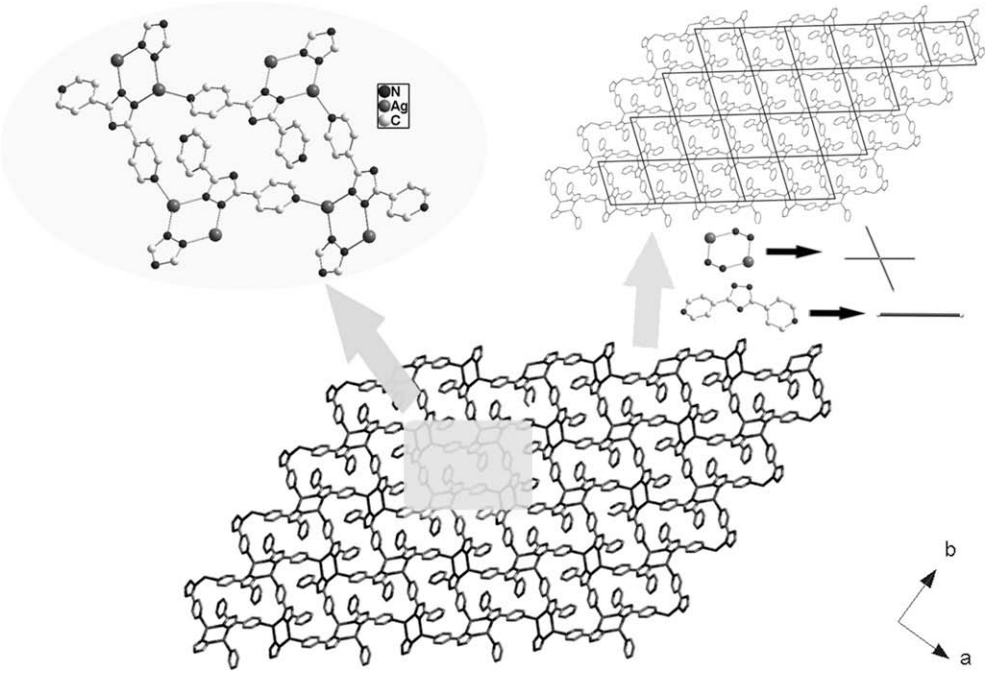

Fig. 7. The two-dimensional (4,4) sheet of compound **4**.

pyridyls of the bpt$^-$ ligands are embedded in this macrocycle. A schematic presentation for the construction of the two-dimensional (4,4) sheet is shown in Fig. 7.

3.2.4. Structure of $[Co(Hbpt)(pa)]_n$ (**4**)

The asymmetric coordination unit of **4** (see Fig. 8a) consists of a pair of Co^{II} ions, one Hbpt, one pa dianion and one aqua ligand. Both crystallographically independent Co^{II} ions lie on inversion centers and display a similar octahedral environment, which are provided by two pyridyl N donors and four carboxylate/water O atoms. As illustrated in Fig. 8b, one carboxylate is monodentate whereas the other adopts a *syn–anti* bridging mode. As a consequence, each Co^{II} ion forms a 7-membered chelated ring with pa, and the adjacent Co^{II} centers are connected by pa components with a separation of 5.245 Å to furnish a polymeric chain along the [0 1 0] direction, with phenyl decorating both sides alternatively. These 1-D arrays are further interlinked through Hbpt spacers to generate a 2-D (4,4) coordination layer along the *bc* plane with a Co···Co separation of 14.237 Å.

Further investigation of the crystal packing reveals that these parallel 2-D arrays are extended via interlayer N2–H2N···O5 interactions (see Table S2 for details) along [1 0 1] to build a 3-D architecture (see Fig. 8c). These hydrogen bonds show a pattern of R_2^2 (18) rings and a large R_2^2 (44) ring [33].

3.2.5. Structure of $[Co(Hbpt)(pda)]_n$ (**5**) and $[Cu(Hbpt)(pda)(H_2O)]_n$ (**6**)

Compounds **5** and **6** display a similar coordination environment as depicted in Fig. 9. Each distorted octahedral Co^{II}/Cu^{II} center is defined by four equatorial oxygen donors and two axial nitrogen atoms from three pda and a pair of Hbpt ligands (see Table S1 for detailed bond parameters). The carboxylate groups in each pda ligand function as a chelated bidentate and in a *syn–syn* bridging mode.

In **5** and **6**, the flexible carboxylate groups ($-CH_2COO^{2-}$) exhibit a *trans* configuration, which has a lesser steric hindrance effect and favors crystal growth [38]. However, the two terminal carboxylates ($-COO^{2-}$) of H_2pda are placed with two different patterns as shown

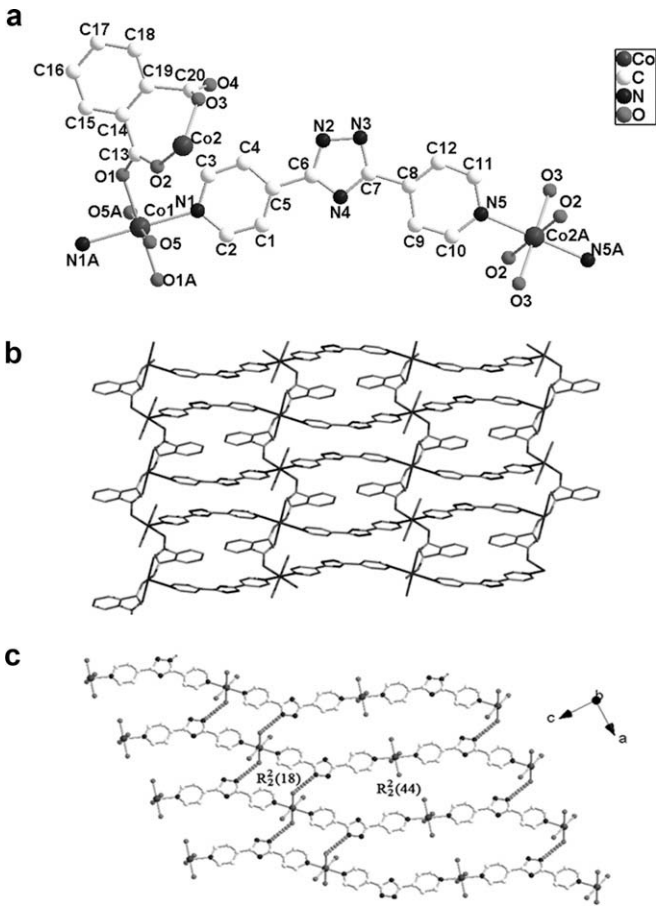

Fig. 8. (a) A portion view of **4** with the atom labelling of the asymmetric unit and Co^{II} coordination. The symmetry code is listed in Table S1. (b) 2-D (4,4) layered coordination framework of **4**. All hydrogen atoms are omitted for clarity. (c) The interlayer hydrogen-bonding interactions construct the 2-D layers into a 3-D network (H-bonds: dashed lines, the phenyl group of the pa ligand was omitted).

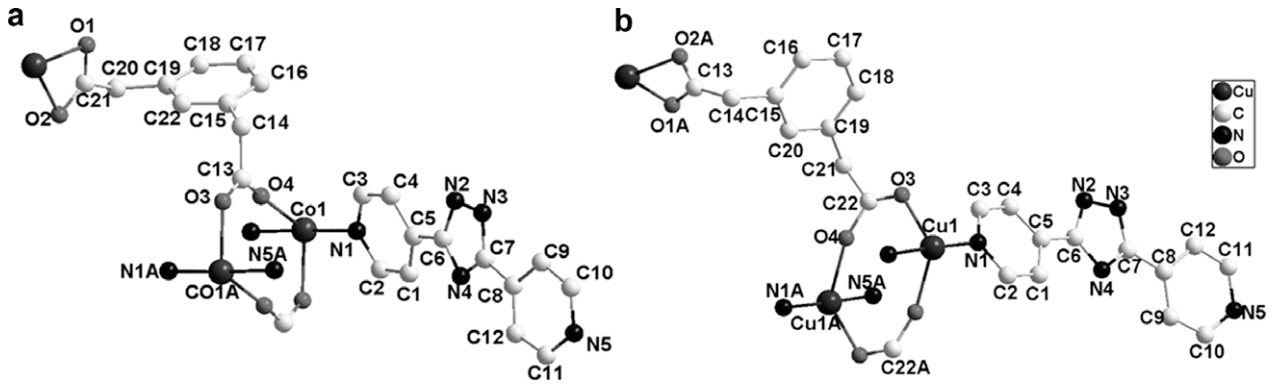

Fig. 9. A portion view of **4** with the atom labelling of the asymmetric unit and Co^{II} coordination. The symmetry code is listed in Table S1: (a) complex **5**; (b) complex **6**.

in Fig. 10, which significantly influences the final 3-D structure of these two similar complexes.

For **5**, as illustrated in Fig. 11a, the carboxylate adopts a chelated bidentate and *syn–syn* mode to bridge the adjacent Co^{II} centers together into a novel two-dimensional sheet parallel to the [1 0 0] plane. The 2-D sheet is composed of two different individual rings. A small dinuclear 7-membered-ring consists of two Co^{II} with two carboxylate groups of pda (Co···Co = 4.118 Å). The larger one comprises a tetrameric unit, in which four dinuclear core Co^{II} centers are linked by pda ligands into an elliptical 40-membered macrocycle. The two-dimensional macrocycle-containing nets can also be represented as a (4,4) net as Fig. 11b. From the *b* axes, the 2-D sheet can further assemble into a 3-D network through Hbpt ligands (Fig. 11c and d). A schematic presentation for the construction of the 3-D network is shown as Fig. 11b and e, the 3-D structure can be simplified as a $(4^{12}\cdot 6^3)$ or α-Po topology.

In **6**, a similar carboxylate group bridges the adjacent Cu^{II} centers together into a novel infinite chain rather than a plane view along the *c* axis; another similar chain is also formed in a different direction, and the pattern of these two similar chains is depicted in Fig. 12c. As shown in Fig. 12b, two Hbpt spacers bridge two adjacent dinuclear cores into a double-strand chain. The chains show an interconnected style as shown in Fig. 12d, the angle between the former two chains and the latter chain is 53.631(1)°. A schematic presentation for the construction of the 3-D network is shown in Fig. 12e, which is very different from **5** and can be simplified as $(6^4\cdot 8^2)$ or $CdSO_4$ topology.

It is also noteworthy that the hydrogen bond of $N_{triazole}$–$H_{triazole}$–O_{pda} links the adjacent Hbpt chains, which further stabilizes the 3-D network. A $R_2^2(18)$ hydrogen bond ring is also found in **6** as depicted in Fig. 13 [33].

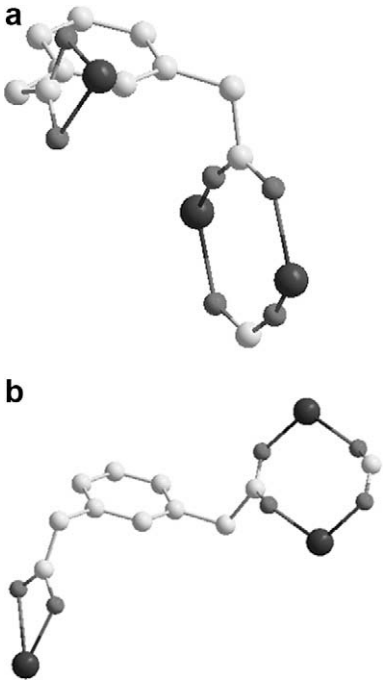

Fig. 10. The two patterns of Hpda in complex **5** (a) and **6** (b).

3.2.6. The coordination modes for the 3,5-bis(4-pyridyl)-1H-1,2,4-triazole ligand

It is noteworthy that Hbpt displays versatile valance states and abundant coordination modes in these metal–organic frameworks. In MOFs **1–6**, the ligand exhibits +2, +1, 0, −1 valance states and several coordination patterns, as illustrated in Schemes 2 and 3, respectively. When Hbpt acts as a neutral ligand, it behaves as a uniform bidentate connector in the 2-D, 3-D coordination networks in **4**, **5** and **6**. While Hbpt present in the form of H_2bpt^+ adopts a monodentate mode in **2**. No coordination action is found in **1** when all the two pyridyls are saturated by protons. An interesting tridentate mode is found in **3** where Hbpt loses the triazole proton.

It is obvious that the introduction of auxiliary dicarboxylate ligands greatly influences the coordination modes of Hbpt as well as the final supramolecular structures. In MOFs **1–3**, Hbpt exhibits abundant coordination modes, whereas it mostly behaves as a uniform bidentate connector in the mixed-ligand complexes **4–6**. In **4–6**, the carboxylate groups adopt the unidentate, chelating and bridging modes, which would be mostly responsible for the structural diversity. In MOFs **4** and **5**, with the variation of the phenyl dicarboxylate building blocks (from pa to pda), their network arrays are changed from 2-D isolated layer (4,4 topology) to 3-D network ($(4^{12}\cdot 6^3)$ topology). On the other hand, the choice of metal center plays a significant role in the resultant networks of MOFs, as shown in **5** and **6**.

The formation of many hydrogen bonds also accompanies the change of Hbpt ligand. In the complexes, except the deprotoned form of **3**, all the hydrogen atoms of the $N_{triazole}$ atoms serve as a donor forming strong hydrogen bonds with oxygen from water or the benzenedicarboxylate ligand with N···O distances ranging from 2.47(2) to 3.23(1) Å [39,40]. The protoned $N_{pyridyl}$ in **1** and **2** also serves as a donor, while the others serve as acceptors in the hydrogen bonds.

3.3. Thermal gravimetric analyses

All the compounds are air stable and can retain their crystallinity at room temperature for at least several weeks. Hence, TGA

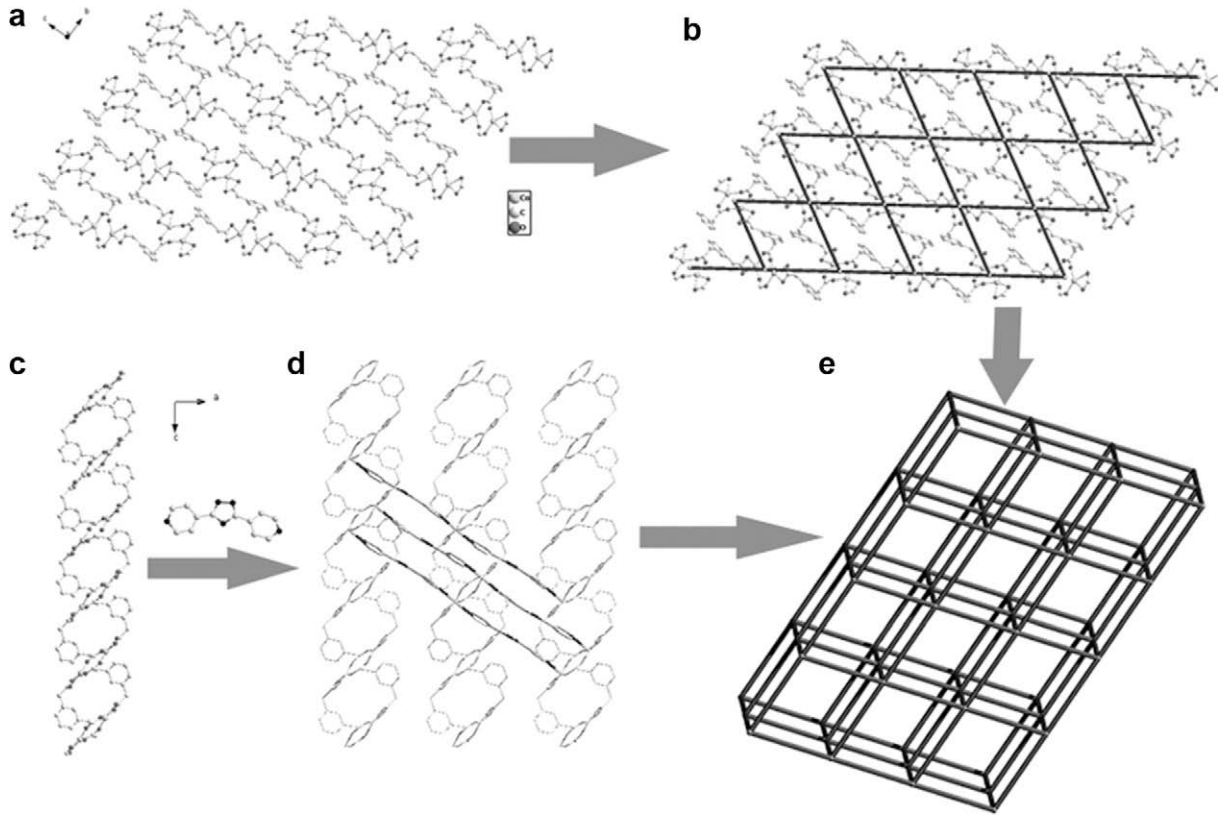

Fig. 11. Construction of the 3-D network for compound **5**: (a) 2-D sheet; (b) simplified 2-D sheet; (c) the 2-D sheet view from the *b* axis; (d) bridge the 2-D to 3-D network; (e) schematic presentation of the $(4^{12} \cdot 6^3)$ network.

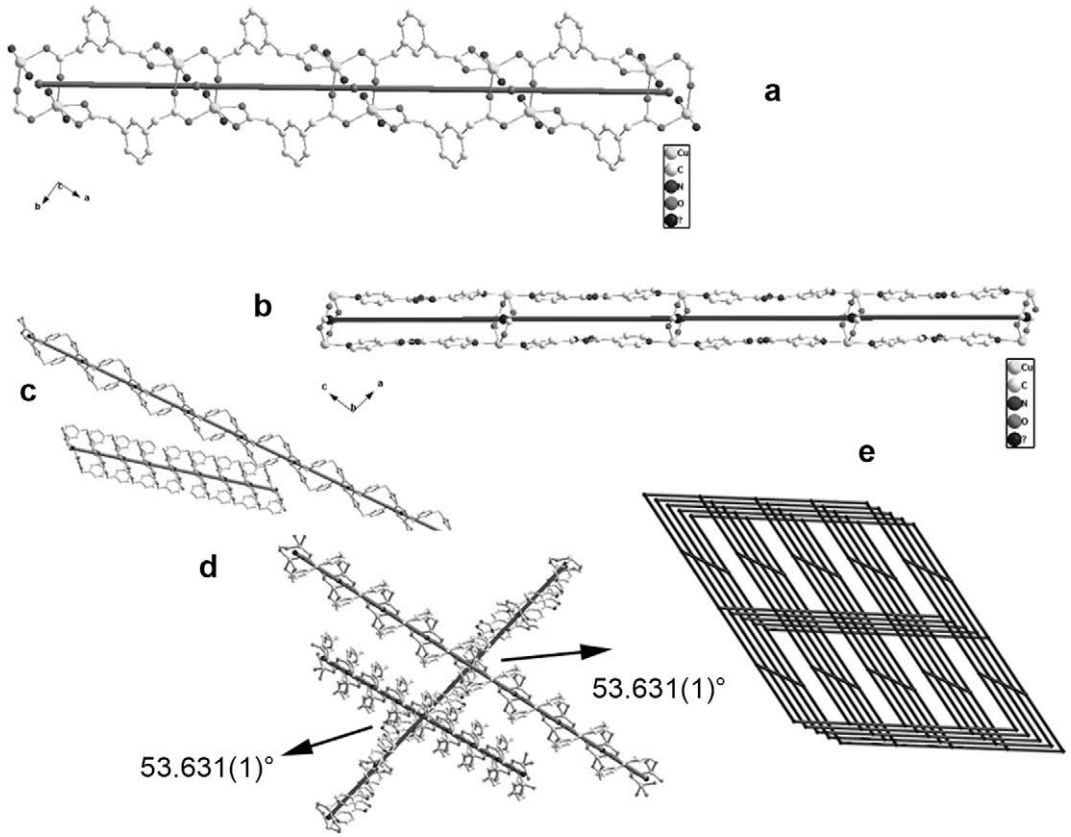

Fig. 12. Construction of the 3-D network for compound **6**: (a) the chain linked by the ip ligand; (b) the double-strand chain linked by bpt; (c) the pattern of the two ip-linked chain; (d) the interconnected style of three chain; (e) schematic presentation of the $(6^4 \cdot 8^2)$ network.

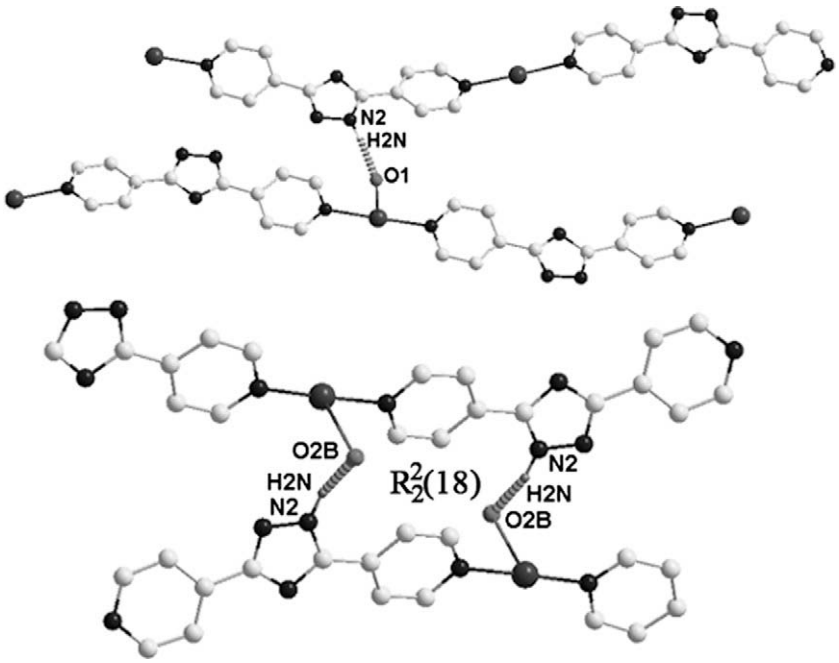

Fig. 13. The hydrogen-bonding interactions for compounds **5** (a) and **6** (b) (H-bonds: dashed lines).

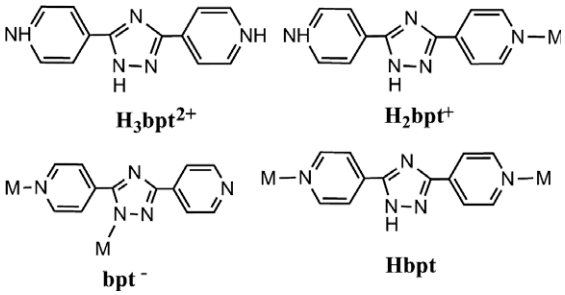

Scheme 3. Coordination modes of the Hbpt ligand in **1**–**6**.

experiments were carried out to explore their thermal stability (see Figs. S1–S5 for TGA curves), which is an important parameter for coordination polymers. **1** quickly loses the free Hbpt ligand and lattice water and is completely converted to the corresponding oxide. In the TGA curve of **2**, the first weight loss of 4.40% in the range 177–243 °C (peak: 227 °C) corresponds to the expulsion of lattice water. The remaining substance is thermally stable up to 310 °C, following that, a series of weight losses occur, which do not end until 810 °C. **3** undergoes consecutive steps of weight loss (peaks: 372.5 and 393.1 °C) from 330.1 °C, which do not stop until 850 °C. For **4**, it remains stable up to 295.5 °C, and then undergoes two step weight losses, corresponding to the loss of the pa and Hbpt ligands, respectively before 675 °C. In **5**, we cannot see two such steps as in **4**, instead a total weight loss from 440 to 750 °C is present. **6** firstly loses the lattice water around 150 °C, and then is stable until 230.5 °C, after that a series of weight losses up to 750 °C are found. In this study, the lattice water molecules in **6** can be facilely excluded upon heating, the residuals have moderate thermal stability. Compound **5** shows the best thermal stability and is stable up to 375 °C, which could be ascribed to the stable 3-D network without lattice guests.

4. Conclusion

In summary, by using the new ligand 3,5-bis(4-pyridyl)-1*H*-1,2,4-triazole (Hbpt), six coordination compounds have been synthesized and characterized. Among them Hbpt exhibits various conformations and adopts different coordinate modes, which may be ascribed to the interactions between the 4-pyridyl and 1*H*-1,2,4-triazole groups. The introduction of dicarboxylate ligands greatly influences the coordination modes of Hbpt as well as the final supramolecular structures. Many hydrogen bonds are formed by the protonated and deprotonated forms of the Hbpt ligand. The results of this study not only illustrate the coordinated behavior of the versatile ligand, but also represent a new inorganic-assisted organic synthesis method. It is anticipated that more metal complexes containing this interesting ligand, as well as more ligands based on this method, will be synthesized.

Acknowledgements

We are grateful to financial support from the National Science Foundation of China (Nos. 20771089, 20873100) and the Natural Science Foundation of Shaanxi Province (Nos. 2007B02, SJ08B09).

Appendix A. Supplementary data

CCDC 697542, 697543, 697544, 697545, 697546 and 697547 contain the supplementary crystallographic data for **1**, **2**, **3**, **4**, **5** and **6**. These data can be obtained free of charge via http://www.ccdc.cam.ac.uk/conts/retrieving.html, or from the Cambridge Crystallographic Data Centre, 12 Union Road, Cambridge CB2 1EZ, UK; fax: (+44) 1223-336-033; or e-mail: deposit@ccdc.cam.ac.uk. Supplementary data associated with this article can be found, in the online version, at doi:10.1016/j.poly.2008.12.046.

References

[1] M. Eddaoudi, D.B. Moler, H.L. Li, B.L. Chen, T.M. Reineke, M. O'Keeffe, O.M. Yaghi, Acc. Chem. Res. 34 (2001) 319.
[2] B. Moulton, M.J. Zaworotko, Chem. Rev. 101 (2001) 1629.
[3] J.S. Seo, D. Whang, H. Lee, S.I. Jun, J. Oh, Y.J. Jeon, K. Kim, Nature 404 (2000) 982.
[4] O.M. Yaghi, M. O'Keeffe, N.W. Ockwig, H.K. Chae, M. Eddaoudi, J. Kim, Nature 423 (2003) 705.
[5] S. Kitagawa, R. Kitaura, S. Noro, Angew. Chem., Int. Ed. 43 (2004) 2334.
[6] H.L. Li, C.E. Davis, T.L. Groy, D.G. Kelley, O.M. Yaghi, J. Am. Chem. Soc. 120 (1998) 2186.

[7] J.P. Zhang, Y.Y. Lin, X.C. Huang, X.M. Chen, Chem. Commun. (2005) 1258.
[8] L.Y. Zhang, J.P. Zhang, Y.Y. Lin, X.M. Chen, Cryst. Growth Des. 6 (2006) 1684.
[9] X.M. Zhang, Z.M. Hao, H.S. Wu, Inorg. Chem. 44 (2005) 7301.
[10] M. Yaghi, H.L. Li, J. Am. Chem. Soc. 118 (1996) 295.
[11] B.H. Ye, M.L. Tong, X.M. Chen, Coord. Chem. Rev. 249 (2005) 545.
[12] Z. Huang, M. Du, H.B. Song, X.H. Bu, Cryst. Growth Des. 4 (2004) 71.
[13] H. Hou, L. Xie, G. Li, T. Ge, Y. Fan, Y. Zhu, New J. Chem. 28 (2004) 191.
[14] X.M. Zhang, R.Q. Fang, H.S. Wu, CrystEngCommun (2005) 96.
[15] M. Du, X.J. Jiang, X.J. Zhao, Inorg. Chem. 45 (2006) 3998.
[16] M. Du, X.J. Jiang, X.J. Zhao, Inorg. Chem. 46 (2007) 3984.
[17] Y.B. Dong, H.Y. Wang, J.P. Ma, R.Q. Huang, M.D. Smith, Cryst. Growth Des. 5 (2005) 789.
[18] A.R. Katritzky, C.W. Rees (Eds.), Comprehensive Heterocyclic Chemistry, vol. 2, Pergamon Press, Oxford, 1997, p. 734.
[19] J.A. McCleverty, T.J. Meyer (Eds.), Comprehensive Coordination Chemistry II, vol. 2, Pergamon Press, Oxford, 1997, p. 425.
[20] M.H. Klingele, S. Brooker, Coord. Chem. Rev. 241 (2003) 119.
[21] S. Horike, S. Bureekaew, S. Kitagawa, Chem. Commun. (2008) 471.
[22] J. Tao, Y. Zhang, M.L. Tong, X.M. Chen, T. Yuen, C.L. Lin, X.Y. Huang, J. Li, Chem. Commun. (2002) 1342.
[23] Y.F. Zhou, R.H. Wang, B.L. Wu, R. Cao, M.C. Hong, J. Mol. Struct. 697 (2004) 73.
[24] K. Uemura, K. Saito, S. Kitagawa, H. Kita, J. Am. Chem. Soc. 128 (2006) 16122.
[25] X.M. Chen, M.L. Tong, Acc. Chem. Res. 40 (2007) 162.
[26] J.P. Zhang, Y.Y. Lin, X.C. Huang, X.M. Chen, J. Am. Chem. Soc. 127 (2005) 5495.
[27] Bruker AXS, SMART, Version 5.0, Bruker AXS, Madison, WI, USA, 1998.
[28] Bruker AXS, SAINT-plus, Version 6.0, Bruker AXS, Madison, WI, USA, 1999.
[29] R.H. Blessing, Acta Crystallogr., Sect. A 51 (1995) 33.
[30] G.M. Sheldrick, Acta Crystallogr., Sect. A 64 (2008) 112.
[31] A.L. Gillon, G.R. Lewis, A.G. Orpen, S. Rotter, J. Starbuck, X.M. Wang, Y. Rodriguez-Martin, C. Ruiz-Perez, J. Chem. Soc., Dalton. Trans. (2000) 3897.
[32] G.A. Jeffrey, H. Maluszynska, Acta Crystallogr., Sect. B 46 (1990) 546.
[33] R.E. Joel Bernstein, D. Liat Shimoni, Ning-Leh Chang, Angew. Chem., Int. Ed. 34 (1995) 1555.
[34] M. Bertelli, L. Carlucci, G. Ciani, D. Proserpio, A. Sironi, J. Mater. Chem. 7 (1997) 1271.
[35] Kaes Christian, M.W.H. Clifton, E.F. Rickard, B.W. Skelton, A.H. White, Angew. Chem., Int. Ed. 37 (1998) 920.
[36] J.P. Zhang, Y.Y. Lin, X.C. Huang, X.M. Chen, Eur. J. Inorg. Chem. (2006) 3407.
[37] J.P. Zhang, Y.Y. Lin, X.C. Huang, X.M. Chen, Inorg. Chem. 44 (2005) 3146.
[38] A.N. Khlobystov, A.J. Blake, N.R. Champness, D.A. Lemenovskii, A.G. Majouga, N.V. Zyk, M. Schroder, Coord. Chem. Rev. 222 (2001) 155.
[39] L. Spek. PLATON, University of Utrecht: Utrecht, the Netherlands, 1998.
[40] A.L. Spek, J. Appl. Crystallogr. 36 (2003) 7.